

## **SUPPORTING INFORMATION**

### **Exciton-Plasmon Interaction between AuNPs/Graphene Nanohybrids and CdS QDs/TiO<sub>2</sub> for Photoelectrochemical Aptasensing of Prostate-Specific Antigen**

**Guoneng Cai, Zhengzhong Yu, Rongrong Ren, and Dianping Tang\***

*Key Laboratory for Analytical Science of Food Safety and Biology (MOE & Fujian Province), State Key  
Laboratory of Photocatalysis on Energy and Environment, Department of Chemistry, Fuzhou University, Fuzhou  
3501168, People's Republic of China*

#### **CORRESPONDING AUTHOR INFORMATION**

Phone: +86-591-2286 6125; fax: +86-591-2286 6135; e-mail: [dianping.tang@fzu.edu.cn](mailto:dianping.tang@fzu.edu.cn) (D. Tang)

## Table of Contents

<b>Experimental Section .....</b>	<b>S3</b>
Reagent and Chemicals .....	S3
Synthesis of Graphene Oxide (GO).....	S3
<b>Partial Experimental Results.....</b>	<b>S4</b>
Figure S1: HRTEM image of CdS QDs/TiO <sub>2</sub> .....	S4
Figure S2: XPS spectra of Ti 2p <sub>3/2</sub> scan, O1s scan and Cd3d <sub>5/2</sub> and Cd3d <sub>3/2</sub> .....	S5
Figure S3: XRD patterns of CdO/TiO <sub>2</sub> .....	S5
Figure S4: TEM image of graphene oxide nanosheets .....	S5
Figure S5: UV-vis absorption spectra and photographs.....	S5
Characterization of the Aptasensing Platform .....	S6
Figure S6: Nyquist diagrams .....	S7
Optimization of Capture DNA-Functionalized AuNPs/GN .....	S7
Figure S7: Effect of C-DNA length and HAuCl <sub>4</sub> amount for preparation of AuNPs/GN .....	S8
REFERENCES .....	S9

## ■ S1. EXPERIMENTAL SECTION

**Reagent and Chemicals.** Cadmium nitrate tetrahydrate [ $\text{Cd}(\text{NO}_3)_2 \cdot 4\text{H}_2\text{O}$ ] and sodium sulfide nonahydrate ( $\text{Na}_2\text{S} \cdot 9\text{H}_2\text{O}$ ) were obtained from Aladdin (Shanghai, China). Poly(alkyleneoxide) block copolymer (Pluronic F-127) was achieved from Sigma-Aldrich (St. Louis, USA). Tris(2-carboxyethyl) phosphine hydrochloride (TCEP) and 6-mercapto-1-hexanol (MCH) were acquired from Tokyo Chem. Inc. (Japan). Graphite powder, ascorbic acid (AA), chloroauric acid ( $\text{HAuCl}_4 \cdot 4\text{H}_2\text{O}$ ), isooctane and titanium tetrachloride ( $\text{TiCl}_4$ ) were purchased from Sinopharm Chem. Re. Inc. (Shanghai, China). PSA standards were acquired from Biocell Biotechnol. Co., Ltd. (Zhengzhou, China). All the oligonucleotides used in this work were from Sangon Biotechnol. Inc. (Shanghai, China), and their sequences were listed as follows:

PSA aptamer: 5'-SH-TTAATTAAAGCTCGCCATCAAATAGC-3'

Capture DNA (C-DNA, 18 nt): 5'-SH-TTTTGCTATTTGATGGCG-3'

Capture DNA (C-DNA, 24 nt): 5'-SH-TTTTTTTTTTGCTATTTGATGGCG-3'

Capture DNA (C-DNA, 30 nt): 5'-SH-TTTTTTTTTTTTTTTTGCTATTTGATGGCG-3'

Capture DNA (C-DNA, 36 nt): 5'-SH-TTTTTTTTTTTTTTTTTTTTGCTATTTGATGGCG-3'

Phosphate-buffered solution (PBS, pH 7.4, containing 0.1 M KCl) was prepared by using 0.1 M  $\text{Na}_2\text{HPO}_4$  and 0.1 M  $\text{NaH}_2\text{PO}_4$ . All other reagents were of analytical grade and used as received without further purification. Ultrapure water obtained from a Millipore water purification system ( $18.2 \text{ M}\Omega \text{ cm}^{-1}$ , Milli-Q) was used in all runs.

**Synthesis of Graphene Oxide (GO).** Graphene oxide was synthesized according to hummer's method with a slight modification.<sup>1</sup> Initially, 2.0 g of graphite powder and 1.0 g of  $\text{NaNO}_3$  were added into the mixture containing 12 mL of the concentrated  $\text{H}_2\text{SO}_4$ , 2.5 g of  $\text{K}_2\text{S}_2\text{O}_8$ , and 2.5 g of  $\text{P}_2\text{O}_5$ . Then, the suspension was kept for 24 h under continuous stirring in an oil bath at 80 °C. Following that, the resulting mixture was carefully diluted with 500-mL ultrapure water, filtered, and washed until the pH of rinse water became neutral. After drying under ambient condition, the pre-oxidized graphite powder was added into another mixture containing 120 mL of the concentrated  $\text{H}_2\text{SO}_4$  and 30 mL of  $\text{HNO}_3$  under continuous stirring. Afterwards, 15 g of  $\text{KMnO}_4$  was added gradually under stirring, followed by cooling down below 20 °C. The resultant mixture was further diluted with 1000 mL of ultrapure water. Subsequently, 20 mL of 30 wt %  $\text{H}_2\text{O}_2$  was added to the mixture, and a brilliant yellow product was formed along with bubbling. After centrifugation,

the precipitate was washed several times with ultrapure water to get a final pH of about 7 and dried at 60 °C for further use.

## ■ S2. PARTIAL EXPERIMENTAL RESULTS

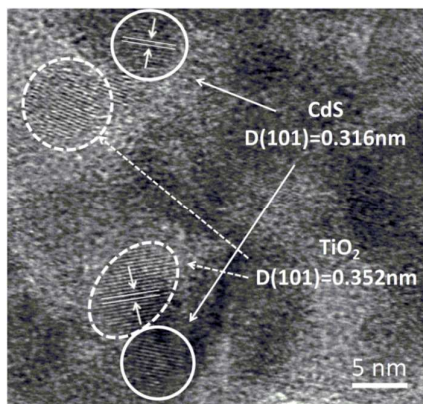


**Figure S1.** HRTEM image of CdS QDs/TiO<sub>2</sub>.

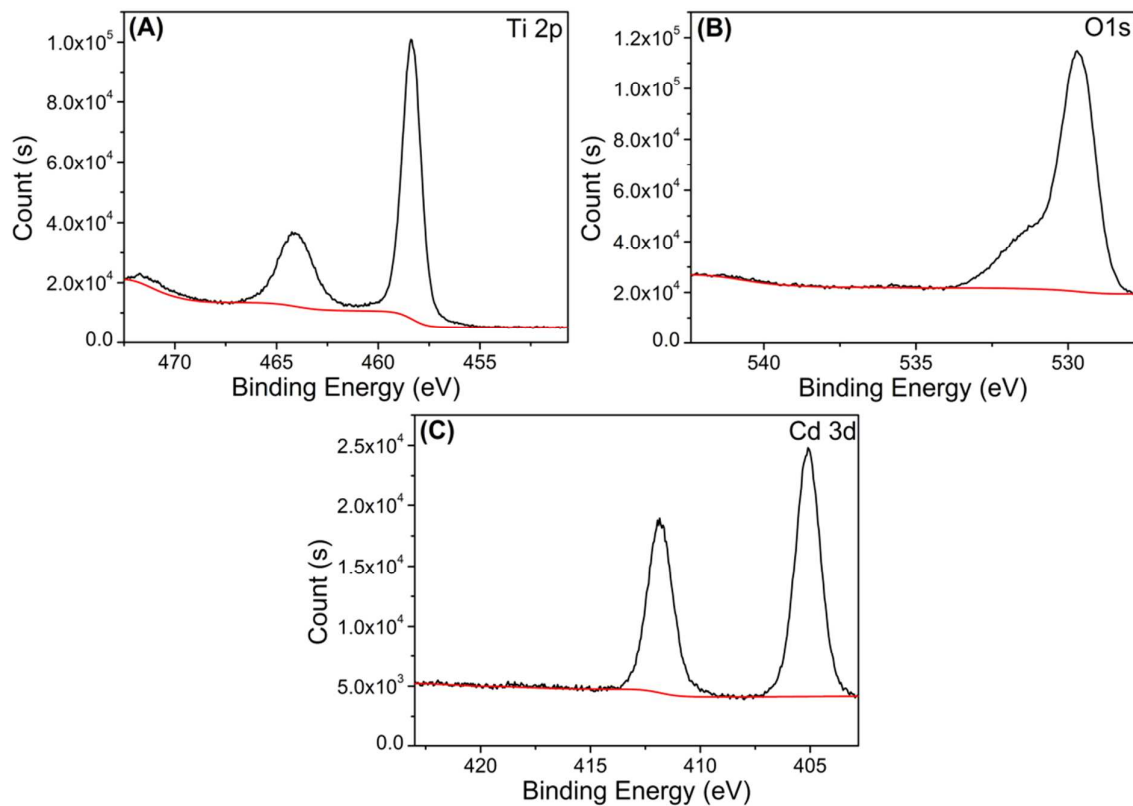


**Figure S2.** XPS spectra of (A) Ti 2p<sub>3/2</sub> scan, (B) O1s scan and (C) Cd3d<sub>5/2</sub> and Cd3d<sub>3/2</sub> in the CdS QDs/TiO<sub>2</sub> sample.

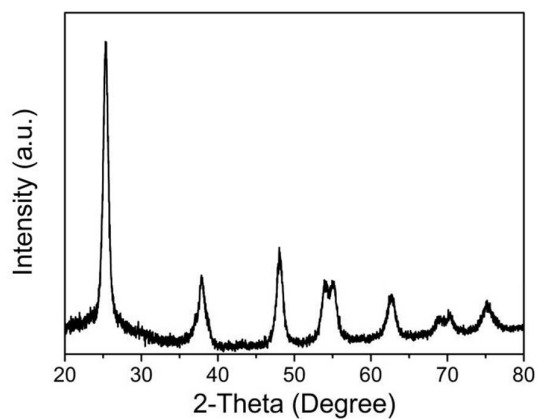


**Figure S3.** XRD patterns of CdO/TiO<sub>2</sub>.

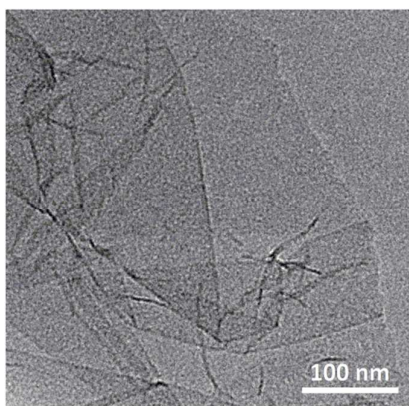


**Figure S4.** TEM image of graphene oxide nanosheets.

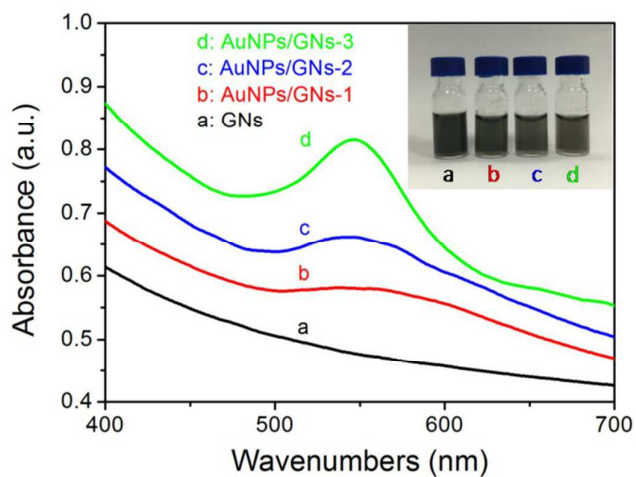


**Figure S5.** UV-vis absorption spectra and photographs (inset) of AuNPs/GN prepared with different-volume HAuCl<sub>4</sub> in 10 mL of the as-synthesized GN suspension (note: GN: 0 uL; AuNPs/GN-1: 50 uL; AuNPs/GN-2: 100 uL; AuNPs/GN-3: 200 uL).

**Characterization of the Aptasensing Platform.** To study the feasibility of the developed aptasensor for target PSA, the electrochemical behaviors after each step by using the as-prepared CdS QDs/TiO<sub>2</sub> and AuNPs/GN were investigated by using electrochemical impedance spectroscopy (EIS) and photocurrent measurement (Figure S6). The Nyquist plots (Figure S6) were used to calculate the electron-transfer resistance ( $R_{ct}$ ).<sup>2</sup> The EIS data were fitted to a Randles equivalent circuit (Figure S6, left inset), which contains electrolyte resistance ( $R_s$ ), the lipid bilayer capacitance ( $CPE$ ), charge transfer resistance ( $R_{ct}$ ) and Warburg element ( $Z_w$ ). The complex impedance can be presented as the sum of the real,  $Z_{re}$  and imaginary,  $Z_{im}$ , components that originate mainly from the resistance and capacitance of the cell. The two components of the scheme,  $R_s$  and  $Z_w$ , represent bulk properties of the electrolyte solution and diffusion of the applied redox probe in solution, respectively. Thus, they are not affected by chemical transformations occurring at the electrode interface. The other two components of the circuit,  $CPE$  and  $R_{ct}$ , depend on the dielectric and insulating features at the electrode/electrolyte interface. In EIS, the semicircle diameter of EIS equals the electron transfer resistance,  $R_{ct}$ . This resistance controls the electron transfer kinetics of the redox-probe at electrode interface. Its value varies when different substances are adsorbed onto the electrode surface. As seen from Figure S6, a small  $R_{ct}$  was obtained at bare FTO electrode (plots 'a'). In contrast, introduction of CdS QDs/TiO<sub>2</sub> on the electrode caused the dramatic increase of the modified electron in the resistance (plots 'b'), which was attributed to the fact that CdS QDs/TiO<sub>2</sub> hindered the transfer of the negatively charged probe of  $[Fe(CN)_6]^{3-/4-}$ . Moreover, the resistance gradually increased when the modified electrode reacted with capture DNA (plots 'c'), MCH (plots 'd'), and PSA aptamer-AuNPs/GN (plots 'e') in sequence. The reason might be the facts that (i) introduction of (bio)molecules/nanomaterials increased the steric hindrance of the sensing interface, and (ii) the negatively charged oligonucleotides hindered the communication of  $Fe(CN)_6^{3-/4-}$  with the base electrode. Favorably, the resistance decreased upon addition of target PSA (plots 'f'). In the presence of target PSA, the analyte initially reacted with the sandwiched aptamer to form the PSA/aptamer complex, thereby resulting in the dissociation of PSA aptamer-AuNPs/GN from the electrode. Just as the partial destruction of the sandwiched structure, the steric hindrance decreased and the electron transfer could accelerate between the redox probe and electrode surface. Moreover, this phenomenon could be clearly observed on the basis of the results obtained by the photocurrents (Figure S6, right inset). Hence, our designed sensing platform could preliminarily apply for

detection of PSA based on target-induced displacement reaction between aptamer-assembled CdS QDs/TiO<sub>2</sub> and AuNPs/GN.

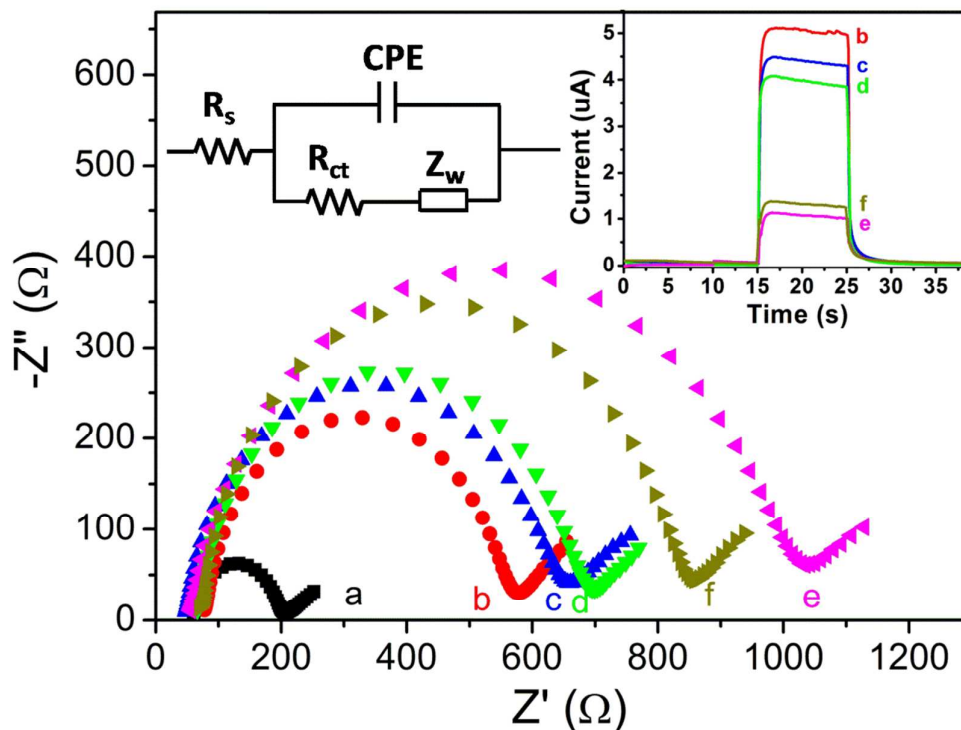


**Figure S6.** Nyquist diagrams of (a) FTO electrode, (b) electrode 'a' + CdS QDs/TiO<sub>2</sub>, (c) electrode 'b' + C-DNA, (d) electrode 'c' + MCH, (e) electrode 'd' + PSA aptamer-AuNPs/GN, and (f) electrode 'e' + PSA in PBS (0.1 M, pH 7.4) containing 0.1 M KCl and 10 mM  $[\text{Fe}(\text{CN})_6]^{3-/4-}$  with the range from 0.1 Hz to  $10^5$  Hz at an alternate voltage of 5 mV (insets: the corresponding photocurrent responses and equivalent circuit).

**Optimization of Capture DNA-Functionalized AuNPs/GN.** In this work, the detectable signal depends on the exciton-plasmon interaction between CdS QDs and AuNPs. Thus, the photocurrent quencher of AuNPs/GN with different-length capture DNA were investigated, *i.e.*, AuNPs/GN-1, AuNPs/GN-2 and AuNPs/GN-3 consisting of different-content AuNPs on the GN. As shown in Figure S7, an optimal quenching effect in the photocurrent was obtained by using 24-nt capture DNA and AuNPs/GN-2 (adding 100  $\mu\text{L}$  of  $\text{HAuCl}_4$  to 10 mL of 0.25 mg/mL GN solution), which was thanks to the interparticle distance between CdS QDs and AuNPs in the EPI systems.<sup>3</sup> Thus, 24-nt capture DNA-functionalized AuNPs/GN-2 were used for the preparation of the aptasensing platform in this work.

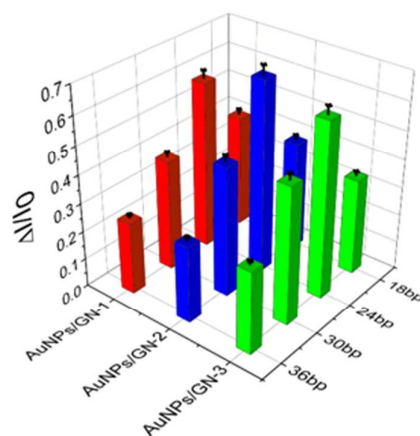


**Figure S7.** The effect of C-DNA length and  $\text{HAuCl}_4$  amount for preparation of AuNPs/GN on the analytical performance of the developed aptasensing platform ( $\Delta I = I_0 - I$ ,  $I_0$  and  $I$  standard for the photocurrents of aptamer/C-DNA/CdS-TiO<sub>2</sub>/FTO electrode before and after incubation with AuNPs/GN, respectively).

## ■ REFERENCES

- (1) Hummers, W.S.; Offeman, R.E. Preparation of graphitic oxide. *J. Am. Chem. Soc.* **1958**, *70*, 1339-1339.
- (2) Zhang, S.; Xia, J.; Li, X. Electrochemical biosensor for detection of adenosine based on structure-switching aptamer and amplification with reporter probe DNA modified Au nanoparticles. *Anal. Chem.* **2008**, *80*, 8382-8388.
- (3) Ma, Z.; Ruan, Y.; Xu, F.; Zhao, W.; Xu, J.; Chen, H. Protein binding bends the gold nanoparticle capped DNA sequence: toward novel energy-transfer-based photoelectrochemical protein detection. *Anal. Chem.* **2016**, *88*, 3864-3871.